Nigerian Journal of Physics (NJP)
ISSN online: 3027-0936
ISSN print: 1595-0611
DOI: https://doi.org/10.62292/njp.v35(s).2026.653
Volume 35(S), 2026

Long-Term Radiological Dose and Cancer Risk Assessment at Hongyum/Pongyum Quarry site, Mpape Using RESRAD-Onsite 7.2

***Celestina Ezekwudo and Raymond Abenga**

Department of Physics, Veritas University Abuja, FCT, Abuja, Nigeria.

*Corresponding Author's Email: ezekwudoc@veritas.edu.ng

Keywords:
RESRAD-Onsite 7.2,
Long-Term Radiological Dose,
NORMs,
Excess Cancer Risk,
NaI(Tl) Spectrometry

Submitted: 20 July 2026

Accepted: 17 Aug. 2026

Published: 09 Sept. 2026

ABSTRACT

The RESRAD-Onsite 7.2 code was applied to assess the long-term total radiological dose and excess cancer risk at the Hongyum/Pongyum Quarry site, Mpape, Federal Capital Territory (FCT), Nigeria, over an area of 183,800 m² and a zone thickness of 2.00 m, for a simulation period of 1.0×10^3 years. Mean activity concentrations of 930.57 ± 61.89 Bq kg^{-1}, 25.34 ± 4.32 Bq kg^{-1}, and 76.28 ± 4.81 Bq kg^{-1} were determined for ^{40}K, ^{226}Ra, and ^{232}Th, respectively using a NaI(Tl) gamma spectrometry system. Concentrations of ^{40}K and ^{232}Th exceeded the UNSCEAR (2000) world average values at all quarry sampling points, while ^{226}Ra remained below the world average at five of the six sampling points. The total dose at t = 0 years for all pathways was $7.878\text{E}-01$ mSv yr^{-1}. The maximum total dose of $1.156\text{E}+00$ mSv yr^{-1} was obtained at t = 37.65 ± 0.08 years, exceeding the Basic Radiation Dose Limit (BRDL) of $1.000\text{E}+00$ mSv yr^{-1}. The total excess cancer risk at t = 0 years was $3.306\text{E}-03$, and a remediation scenario using a 1.25 m clean soil cover reduced the total dose by 82.6% and the total excess cancer risk by 85.5%. The Hongyum/Pongyum Quarry site presents an unacceptable radiological cancer burden under current unmitigated conditions. While the 1.25 m clean soil cover is an effective first remediation step, supplementary radon attenuation measures are required alongside the soil cover to bring the site within the WHO-acceptable cancer risk threshold.

INTRODUCTION

Exposure of the general public to ionizing radiation from both natural and human-made sources cannot be completely avoided (ICRP, 2007). Naturally occurring radiation sources are inherent components of the environment and cannot be eliminated; consequently, controlling excessive inhalation or accumulation through systematic radiological assessments is essential for public health protection. The assessment of radiological risks associated with naturally occurring radioactive materials (NORMs) at quarry and mining sites has become a global public health priority, particularly in developing countries where regulatory oversight of extractive industries is often limited (Abdu et al., 2024; Ofomola et al., 2023). A primary consideration in formulating key environmental decisions and policies depends on potential risk to human health and the environment (Bellamy et al., 2014). Quarrying operations disrupt geological strata, mechanically disaggregate rocks, and bring naturally occurring radionuclides — principally ^{40}K, ^{226}Ra, and ^{232}Th — to the surface, enhancing their bioavailability and mobility in the environment (Jegede et al., 2025; Farai, 2007). Workers, nearby residents, and populations dependent on food crops and groundwater from such areas are potentially exposed through multiple radiological pathways, including external gamma irradiation, inhalation of radon and its decay products, ingestion of contaminated soil, and consumption of plant foods, meat, milk, and drinking water (Muhammad et al., 2024; UNSCEAR, 2000).

In Nigeria, quarrying activities are widespread and often conducted without comprehensive radiological baseline assessments or formal risk-management frameworks (Bello et al., 2022; Girigisu et al., 2013). Several studies have documented elevated NORM concentrations at quarry sites across Nigeria (Jegede et al., 2025; Ofomola et al., 2023), with findings consistently showing that ^{40}K frequently exceeds the UNSCEAR (2000) world average of 400 Bq kg^{-1}. Elevated ^{232}Th at Nigerian quarry sites

has been attributed to the lithological character of the Basement Complex rocks, which are enriched in thorium-bearing accessory minerals such as monazite and zircon (Ofomola et al., 2023; Farai, 2007). Air quality assessments around the Mpape quarry in Abuja have also documented elevated SO_2 and NO_2 levels associated with quarry blasting and crushing operations (Omeiza et al., 2022), highlighting the broader environmental impacts of quarrying in this area.

The Hongyum Quarry, located in Mpape, Federal Capital Territory (FCT), Nigeria, is one of the most active granite quarrying sites in the FCT, supplying construction materials for Abuja's ongoing infrastructural development (Omeiza et al., 2022). The surrounding community is in proximity to quarrying operations, relies on local groundwater and food crops, and has not been subject to any known prior long-term radiological dose and cancer risk assessment, although background radiation and associated risk have previously been assessed at other public sites within the FCT (Ojo et al., 2024). The present study fills this gap by applying the RESRAD-Onsite 7.2 code to estimate radionuclide transport, long-term dose accumulation, and excess cancer risk at this site. RESRAD-Onsite 7.2, developed by Argonne National Laboratory under the United States Department of Energy (DOE), is a widely used deterministic environmental dose assessment tool applied in comparable NORM assessments (Abdu et al., 2024; Njinga & Tshivhase, 2018; Yu et al., 2001b).

This study analyses the activity concentration of ^{232}Th, ^{226}Ra, and ^{40}K over an area of 183,800 m² and shows how the *K*d values of ^{232}Th, ^{226}Ra, and ^{40}K for the loamy sand to sandy loam soil type contribute to the peak dose in the affected zone. Furthermore, the pathway contributions to the peak dose over the span of 1000 years were evaluated, and the excess lifetime cancer risk was calculated. Finally, the study evaluates how the site could be remediated using a clean cover layer of 1.25 m (depth) of soil so that the area could be returned to farming and other basic activities with reduced radiological health risk to the surrounding population. The specific objectives of this study are to: determine the activity concentrations of ^{40}K, ^{226}Ra, and ^{232}Th in soils from the Hongyum/Pongyum Quarry site and a reference control site; evaluate individual and summed pathway contributions to total radiological dose over a 1000-year simulation horizon; quantify the excess lifetime cancer risk attributable to each radionuclide and pathway; and model the effectiveness of a 1.25 m clean soil cover as a remediation strategy.

MATERIALS AND METHODS

Study Area

Hongyum/Pongyum Quarry site is located in Mpape, Bwari Area Council, Federal Capital Territory (FCT), Abuja, Nigeria (Latitude 9.1350° N; Longitude 7.4989° E). Mpape is a rapidly growing peri-urban community with an estimated population of over 100,000. The site lies within the Nigerian Basement Complex, characterised by Precambrian crystalline rocks including granite gneisses, migmatites, and schists (Omeiza et al., 2022). These geological formations are known to be enriched in naturally occurring radionuclides, particularly ^{232}Th and ^{40}K associated with potassium feldspar and thorium-bearing accessory minerals (Farai, 2007; Ofomola et al., 2023). The soils of the study area are classified as loamy sand to sandy loam, with a mineral composition dominated by potassium feldspar, quartz, and biotite mica. Surrounding communities depend on hand-dug wells and boreholes for domestic water supply, and food crops including maize, leafy vegetables, and yam are cultivated on adjacent lands, making multi-pathway radiological dose assessment critically important. A map of the study area showing the quarry site and sampling locations is presented in Figure 1.

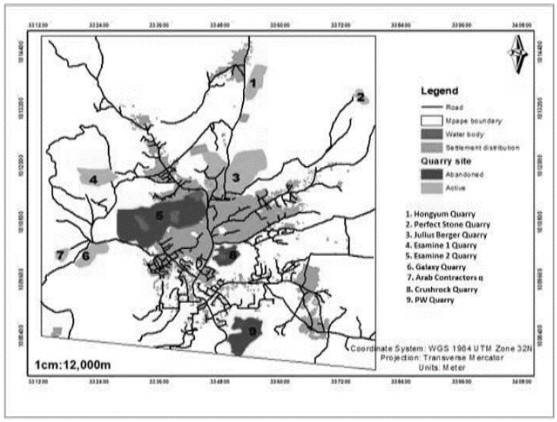

Figure 1: Map of the Quarry Site in the Study Area.
Source: NAGIS (2018)

Soil Sample Collection

Six sampling points (QPT1–QPT6) were systematically established within the active quarrying zone, and one control site was selected at a location with no history of quarrying or industrial activity, following internationally accepted soil sampling protocols for radioactivity studies (IAEA, 1989; Muhammad et al., 2024). At each sampling point, a 0.5 m × 0.5 m area was demarcated and cleared of surface debris to a depth of 0.30 m. Approximately 2 kg of soil was collected with a stainless-steel auger at a depth of 0.15 m below the cleared surface to capture the natural soil horizon. All samples were labelled with GPS coordinates and transported to the laboratory in sealed polythene bags to prevent cross-contamination.

In the laboratory, soil samples were air-dried, crushed with a mortar and pestle, and sieved through a 0.2-mm mesh to obtain a homogeneous fine powder. Each powdered sample was oven-dried at 383 K for 24 hours to remove residual moisture, then packed into radon-impermeable cylindrical plastic containers of 76 × 76 mm dimension — matching the detector geometry — and triple-sealed to prevent ^{222}Rn escape: the inner rim of each container lid was smeared with Vaseline jelly, the lid-container gap was filled with candle wax, and the assembly was further secured with masking adhesive tape. Samples were stored for a minimum of 30 days before counting to achieve secular radioactive equilibrium between radon (^{222}Rn), thoron (^{220}Rn), and their respective short-lived progeny — a prerequisite for accurate determination of ^{226}Ra via ^{214}Bi and ^{232}Th via ^{208}Tl (Abdu et al., 2024; Muhammad et al., 2024).

NaI(Tl) Spectrometry and Detector Calibration

Radioactivity measurements were performed using a NaI(Tl) scintillation detector with a crystal dimension of 76 × 76 mm (3″ × 3″), optically coupled to a photomultiplier tube (PMT) with an incorporated preamplifier and a 1 kV external power supply (CANBERRA Model 727, Serial No. 11914167). The detector assembly was enclosed in a 6 cm lead shield lined with cadmium and copper sheets to minimise contributions from background and scattered radiation. Spectral data were acquired using MAESTRO data acquisition software (Canberra Nuclear Products) for a counting period of 28,800 s per sample. Background spectra were acquired for 28,800 s and subtracted from all sample spectra. Although HPGe detectors offer superior energy resolution, NaI(Tl) scintillation systems have been widely validated for NORM quantification in environmental soil matrices using the three-window method employed here, and have been used in comparable radiological assessments at Nigerian quarry and mining sites (Abdu et al., 2024; Muhammad et al., 2024; Ofomola et al., 2023). The use of IAEA standard reference materials (RGK-1, RGU-1, RGTh-1) further ensured the reliability of the measurements.

Energy and efficiency calibrations were performed using two-point calibration sources — ^{137}Cs (661.6 keV) and ^{60}Co (1173 keV and 1332 keV) — with the amplifier gain adjusted to achieve 7.2% energy resolution (FWHM) at the 661.6 keV peak of ^{137}Cs, counted for 30 minutes. IAEA standard reference materials — RGK-1 (^{40}K), RGU-1 (^{226}Ra via ^{214}Bi peak), and RGTh-1 (^{232}Th via ^{208}Tl peak) — were prepared in identical cylindrical container geometry and used to verify calibration. The spectral energy windows and calibration factors used in the analysis are given in Table 1.

Table 1: Spectral Energy Windows and Calibration Factors Used in NaI(Tl) Analysis

Radionuclide	Gamma Energy (keV)	Energy Window (keV)	Calibration Factor C_{fk} (×10^{-3} cps(ppm)$^{-1}$)
^{226}Ra	1764.0	1620–1820	10.500
^{232}Th	2614.5	2480–2820	3.612
^{40}K	1460.0	1380–1550	0.026

Note: Detection Limits: 40K = 14.54 Bq kg^{-1}; 226Ra = 3.84 Bq kg^{-1}; 232Th = 9.08 Bq kg^{-1}. Calibration Factors from the CANBERRA Model 727 System Calibration

Determination of Activity Concentrations

The activity concentration of each radionuclide in the soil samples was determined from the net count rate under selected gamma-ray photo peaks using Equation 1 (Daburum et al., 2023; Abdu et al., 2024):

$$C\ (\text{Bq}\ kg^{-1}) = \frac{C_n}{C_{fk}} \quad (1)$$

where C is the activity concentration of the radionuclide in the sample (Bq kg^{-1}); C_n is the net count rate (counts per second, cps), calculated as Equation 2:

$$C_n(\text{cps}) = \frac{Net\ Counts}{Live\ Time(s)} \quad (2)$$

and C_{fk} is the calibration factor of the NaI(Tl) detection system for the respective radionuclide (Table 1). The activity concentration of ^{226}Ra was determined from the 1764.0 keV gamma line of ^{214}Bi (energy window: 1620–1820 keV). The ^{232}Th concentration was determined from the 2614.5 keV gamma line of ^{208}Tl (energy window: 2480–2820 keV). The ^{40}K concentration was derived from its 1460.0 keV gamma transition (energy window: 1380–1550 keV).

Quality Assurance and Quality Control

Rigorous quality control was maintained throughout the analytical procedure. Detector background spectra were acquired regularly and subtracted from all sample spectra. The IAEA standard reference materials (RGK-1, RGU-1, and RGTh-1) were analysed using the same procedure as the samples, and measured values were compared against IAEA-certified reference values. Satisfactory agreement was achieved for all three radionuclides, confirming the reliability of the analytical procedure. Detection limits were 14.54 Bq kg^{-1} for ^{40}K, 3.84 Bq kg^{-1} for ^{226}Ra, and 9.08 Bq kg^{-1} for ^{232}Th.

Rate of Radionuclide Release from the Contaminated Zone

In RESRAD-Onsite 7.2, the release rate of radionuclides from the contaminated soil zone is governed by a nuclide-specific, first-order leach rate constant. This approach accounts for the partitioning of radionuclides between the soil solid phase and pore water, as quantified by the soil-water distribution coefficient (*K*d). The radionuclide release rate for species i is given by Equation 3 (Yu et al., 2001b; Njinga & Tshivhase, 2018):

$$\frac{dR_i(t)}{dt} = L_i * \rho b * A * T(t) * S_i(t) \qquad (3)$$

where L_i is the first-order leach rate constant for radionuclide i (yr^{-1}); ρb is the bulk density of the contaminated zone (kg m^{-3}); A is the area of the contaminated zone (m^2); $T(t)$ is the thickness of the contaminated zone at time t (m); and $S_i(t)$ is the mean concentration of the ith principal radionuclide available for leaching at time t (Bq g^{-1}).

The first-order leach rate constant used in RESRAD is a time-independent radionuclide leach rate constant. It is estimated based on the soil residence time for the initial thickness of the contaminated zone and is given by Equation 4 (Njinga & Tshivhase, 2018):

$$L_i = \frac{I}{V_{wc} \times T_0 \times R_f} = \frac{(1 - C_e) \times [P_r \times (1 - C_r) + I_r]}{V_{wc} \times T_0 \times R_f} \qquad (4)$$

where I = infiltration rate (m/yr); V_{wc} = volumetric water content of the contaminated zone (= V_{wc}s × R$_s$); V_{wc}s = saturated water content (= total porosity P_t); T_0= initial thickness of the contaminated zone (m); R_f = retardation factor for radionuclide i; C_e = evapotranspiration coefficient; C_r = runoff coefficient; P_r = precipitation rate (m/yr); I_r = irrigation rate (m/yr).

When the medium is saturated, the saturation ratio of the contaminated zone Rs equals unity (Rs = 1). Under unsaturated infiltration conditions, the saturation ratio is a function of the infiltration rate, the saturated hydraulic conductivity, and soil texture. The saturation ratio can be estimated using Equation 5 (Clapp & Hornberger, 1978; Njinga & Tshivhase, 2018),

$$R_s = \left(\frac{I}{H_C^S}\right)^{\frac{1}{2b+3}} \qquad (5)$$

where H_C^S = saturated hydraulic conductivity (myr^{-1}); b = soil-specific exponential parameter.

The retardation factor Rfi for radionuclide i is the ratio of the average pore water velocity to the radionuclide transport velocity. Assuming a linear adsorption–desorption isotherm, it is given by Equation 6 (Njinga & Tshivhase, 2018; Yu, 1987; Yu, 1999):

$$R_{f_i} = 1 + \frac{\rho_b \times k_{d_i}}{V_{wc}} = 1 + \frac{\rho_b \times k_{d_i}}{P_t \times R_s} \qquad (6)$$

where k_{d_i} = distribution coefficient for the i^{th} principal radionuclide (cm^3 g^{-1}); ρ_b = bulk density (g cm^{-3}); P_t= total porosity. The leaching rate of a radionuclide is determined by its k_{d_i} value, which governs the relative transport velocity of the radionuclide compared to water in the pore space. The leach rate also depends on the infiltration rate, soil properties (bulk density, porosity, saturated hydraulic conductivity, b-parameter), and contamination extent (zone thickness, area, and radionuclide concentration).

RESRAD-Onsite 7.2 Input Parameters

The RESRAD-Onsite 7.2 simulation was configured using the ICRP Publication 107 (ICRP, 2008) nuclear decay data library, Federal Guidance Reports FGR-11 and FGR-12 for internal and external dose conversion factors, respectively, and FGR-13 for carcinogenic risk coefficients. A radionuclide half-life cut-off of 180 days was applied. The simulation spanned 1000 years (1.0 × 10^3 yr). Two scenarios were modelled: the unmitigated condition with cover depth = 0.00 m, and the remediation scenario with a 1.25 m clean soil cover. Mean activity concentrations from Table 3b were used as primary RESRAD inputs: 0.93057 Bq g^{-1} (^{40}K), 0.02534 Bq g^{-1} (^{226}Ra), and 0.07628 Bq g^{-1} (^{232}Th). Site-specific and default input parameters are summarised in Table 2. The distribution coefficients (K_d values) of Ra-226, Th-232 and K-40 across the three zones (contaminated, saturated and unsaturated) were set to 36,000 cm^3 g^{-1}, 3,300 cm^3 g^{-1}, and 55 cm^3 g^{-1}, respectively, for loamy sand to sandy loam soils, following the values reported by Njinga and Tshivhase (2018) for texturally comparable Basement Complex soils, in order to evaluate the transport mechanism to the water table.

Table 2: Site-Specific and Default Input Parameters Used in RESRAD-Onsite 7.2 Simulations

Parameter	Site-Specific Data	Default Value
Area of contaminated zone	183,800 m² (0.1838 km²)	—
Thickness of contaminated zone	2.00 m	—
Cover depth (Scenario 1 / Scenario 2)	0.00 m / 1.25 m	—
Density of contaminated zone	1.44 g/cm³	—
Contaminated zone total porosity	0.43	—
Contaminated zone b-parameter	4.9	—
Evapotranspiration coefficient	—	0.5
Contaminated zone erosion rate	—	0.001 m/yr
Wind speed	4.1 m/s	—
Precipitation rate	1.0 m/yr	—
Irrigation rate	—	0.2 m/yr
Saturated zone total porosity	—	0.4
Saturated zone effective porosity	—	0.2
Saturated hydraulic gradient	—	0.02
Saturated zone b-parameter	—	5.3
Water table drop rate	—	0.001 m/yr
Well pump intake depth	10 m	—
Exposure duration	30 years	—
Simulation time span	1000 years	—
Indoor time factor	0.5	—
Outdoor time factor	0.3	—
Fruits and grains consumption rate	—	160 kg/yr
Leafy vegetable consumption rate	—	14 kg/yr
Soil ingestion rate	37 g/yr	—
Drinking water intake	—	510 litres/yr
Half-life cut-off	180 days	—
Dose library	FGR 11, 12 & 13; ICRP-38	—
Basic Radiation Dose Limit (BRDL)	1.000E+00 mSv/yr	—

Note: Site-Specific Values from Field Measurements and Site Characterisation. Default Values from Yu et al. (2001a);Yu et al. (2001b). BRDL as Applied by the Code = 1.000E+00 mSv/yr

RESULTS AND DISCUSSION

Activity Concentrations and Comparison with World Average

The measured activity concentrations of ^{40}K, ^{226}Ra, and ^{232}Th in soil samples from the six quarry sampling points and the control site are presented in Table 3a, and their conversion to Bq g^{-1} for use as RESRAD-Onsite 7.2 primary inputs are given in Table 3b. At the quarry site, mean activity concentrations were 930.57 ± 61.89 Bq kg^{-1} (^{40}K), 25.34 ± 4.32 Bq kg^{-1} (^{226}Ra), and 76.28 ± 4.81 Bq kg^{-1} (^{232}Th). The control site yielded substantially lower values of 71.28 ± 5.63 Bq kg^{-1} (^{40}K), 31.94 ± 2.09 Bq kg^{-1} (^{226}Ra), and 15.84 ± 1.26 Bq kg^{-1} (^{232}Th), confirming enhancement of ^{40}K and ^{232}Th radioactivity at the quarry site relative to the uncontaminated background, consistent with mechanical exposure and disaggregation of thorium- and potassium-bearing minerals during quarrying. It is noteworthy that the control site recorded a higher ^{226}Ra concentration (31.94 ± 2.09 Bq kg^{-1}) than the quarry site mean (25.34 ± 4.32 Bq kg^{-1}). This is consistent with observations in other Basement Complex terrains where undisturbed soils can retain uranium-series radionuclides through sorption onto iron oxides and clay minerals, while quarrying-induced mechanical disaggregation and surface runoff at the active site may mobilise and partially remove ^{226}Ra from the sampling horizon (Farai, 2007; Bello et al., 2022). The elevated ^{232}Th and ^{40}K at the quarry relative to the control site nevertheless confirm net NORM enhancement from quarrying operations.

Comparing with UNSCEAR (2000) world average values — 400 Bq kg^{-1} (^{40}K), 35 Bq kg^{-1} (^{226}Ra), and 30 Bq kg^{-1} (^{232}Th) — all six quarry sampling points recorded ^{40}K and ^{232}Th concentrations above the world average, ranging from 718.42 to 1110.05 Bq kg^{-1} and 59.27 to 95.57 Bq kg^{-1}, respectively. ^{226}Ra remained below the world average at five of the six points, except for QPT6 (46.19 ± 3.88 Bq kg^{-1}), which likely reflects localised geological enrichment or preferential mobilisation of ^{226}Ra from uranium-series mineral phases at that quarrying face (Bello et al., 2022; Farai, 2007). These findings are consistent with studies from other Nigerian granite quarry sites (Ofomola et al., 2023; Jegede et al., 2025).

Table 3a: Activity Concentrations of ^{40}K, ^{226}Ra, and ^{232}Th in Soil Samples

S/No	Location	^{40}K (Bq kg^{-1})	Status	^{226}Ra (Bq kg^{-1})	Status	^{232}Th (Bq kg^{-1})	Status
1	QPT1	989.99 ± 11.09	Above	19.63 ± 1.89	Below	72.47 ± 3.59	Above
2	QPT2	866.27 ± 10.40	Above	25.66 ± 1.99	Below	80.09 ± 4.43	Above
3	QPT3	828.37 ± 9.47	Above	20.43 ± 2.29	Below	75.23 ± 3.26	Above
4	QPT4	1070.30 ± 10.73	Above	22.56 ± 1.03	Below	95.57 ± 4.68	Above
5	QPT5	1110.05 ± 11.79	Above	17.54 ± 1.85	Below	75.03 ± 3.95	Above
6	QPT6	718.42 ± 9.91	Above	46.19 ± 3.88	Above	59.27 ± 3.76	Above
7	Control Site	71.28 ± 5.63	Below	31.94 ± 2.09	Below	15.84 ± 1.26	Below
	Minimum	71.28	—	17.54	—	15.84	—
	Maximum	1110.05	—	46.19	—	95.57	—
	SE (Quarry)	61.89	—	4.32	—	4.81	—
	Mean (Quarry)	930.57 ± 61.89	ABOVE	25.34 ± 4.32	BELOW	76.28 ± 4.81	ABOVE

Note: Status Denotes Comparison with UNSCEAR (2000) World Average: ^{40}K = 400, ^{226}Ra = 35, ^{232}Th = 30 Bq kg^{-1}. SE = Standard Error from Quarry Points QPT1–QPT6 only

Table 3b: Mean Activity Concentrations in Bq kg^{-1} and Bq g^{-1} Used as Primary RESRAD-Onsite 7.2 Inputs

Location	^{40}K (Bq kg^{-1})	^{40}K (Bq g^{-1})	^{226}Ra (Bq kg^{-1})	^{226}Ra (Bq g^{-1})	^{232}Th (Bq kg^{-1})	^{232}Th (Bq g^{-1})
QPT1	989.99	0.98999	19.63	0.01963	72.47	0.07247
QPT2	866.27	0.86627	25.66	0.02566	80.09	0.08009
QPT3	828.37	0.82837	20.43	0.02043	75.23	0.07523
QPT4	1070.30	1.07030	22.56	0.02256	95.57	0.09557
QPT5	1110.05	1.11005	17.54	0.01754	75.03	0.07503
QPT6	718.42	0.71842	46.19	0.04619	59.27	0.05927
Control	71.28	0.07128	31.94	0.03194	15.84	0.01584
Mean	930.57	0.93057	25.34	0.02534	76.28	0.07628
World Avg	400.00	—	35.00	—	30.00	—

Note: Conversion: 1 Bq kg^{-1} = 1 × 10^{-3} Bq g^{-1}. Bold row = Mean Values Used as RESRAD Simulation Inputs. World Average from UNSCEAR (2000)

Total Dose Assessment at t = 0 Years

The total radiological dose contributions at t = 0 years, disaggregated by radionuclide and pathway, are presented in Table 4. The total dose across all nuclides and pathways at t = 0 was 7.878E-01 mSv yr^{-1}, below the BRDL of 1.000E+00 mSv yr^{-1} but substantially exceeding the ICRP (1990) public dose limit of 0.25 mSv/yr. ^{40}K dominated the total dose at t = 0, contributing 5.155E-01 mSv yr^{-1} (65.44%), followed by ^{226}Ra at 2.540E-01 mSv yr^{-1} (32.24%) and ^{232}Th at 1.826E-02 mSv yr^{-1} (2.32%).

The ground (external gamma) pathway delivered the highest dose of 2.009E-01 mSv yr^{-1} (25.50%), followed by radon at 1.917E-01 mSv yr^{-1} (24.33%), plant ingestion at 1.863E-01 mSv yr^{-1} (23.65%), and meat ingestion at 1.526E-01 mSv yr^{-1} (19.37%). Milk contributed 6.504E-02 mSv yr^{-1} (8.26%), while inhalation and soil ingestion were negligible (4.371E-04 and 1.016E-03 mSv yr^{-1}, respectively). Water-dependent pathways contributed zero dose at t = 0, consistent with the high K_d values for all three radionuclides, which retard transport to the water table (Gil-García et al., 2009).

Table 4: Total Dose Contributions TDOSE(i,p,t) for Individual Radionuclides and Pathways at t = 0 Years (mSv yr^{-1})

Nuclide	Ground	Inhalation	Radon	Plant	Meat	Milk	Soil	All Pathways
^{40}K	1.529E-01	3.906E-06	0.000E+00	1.492E-01	1.506E-01	6.261E-02	1.693E-04	5.155E-01
^{226}Ra	4.361E-02	1.218E-05	1.916E-01	2.548E-02	1.511E-03	1.793E-03	2.323E-04	2.540E-01
^{232}Th	4.400E-03	4.210E-04	5.731E-05	1.161E-02	5.189E-04	6.331E-04	6.147E-04	1.826E-02
Total	2.009E-01	4.371E-04	1.917E-01	1.863E-01	1.526E-01	6.504E-02	1.016E-03	7.878E-01

Note: Inhalation Excludes Radon. Water-Dependent Pathway Contributions were Zero for all Nuclides at t = 0. All Values in mSv yr^{-1}. From RESRAD-Onsite 7.2 Output File SITE4.RAD

Maximum Total Dose and Time-Dependent Dose Evolution

The temporal evolution of total radiological dose over the 1000-year simulation horizon is presented in Table 5 and illustrated in Figure 2. The maximum total dose (t-max-D) was 1.156E+00 mSv yr^{-1}, occurring at t = 37.65 ± 0.08 years — exceeding the BRDL of 1.000E+00 mSv yr^{-1} and confirming that the site poses an unacceptable long-term radiological risk under current unmitigated conditions. Nuclide and pathway contributions at t-max-D are detailed in Table 5.

At t = 37.65 years, ^{40}K remained the dominant contributor (4.830E-01 mSv yr^{-1}; 41.79%), while ^{232}Th increased substantially from 1.826E-02 mSv yr^{-1} (2.32%) at t = 0 to 3.913E-01 mSv yr^{-1} (33.85%) at t-max-D. This dramatic rise in ^{232}Th dose is attributable to the ingrowth of its decay chain progeny, principally ^{228}Ra, ^{228}Th, and ^{228}Ac, which accumulate over time and contribute significantly through ground irradiation and plant ingestion pathways (Muhammad et al., 2024; Yu et al., 2001a). ^{226}Ra contributed 2.815E-01 mSv yr^{-1} (24.35%) at t-max-D. These dynamics underscore the importance of long-term simulation rather than merely reporting the t = 0 value, as dose increases substantially over decadal timescales before declining as radionuclides are depleted through decay, erosion, and leaching. The contributions of individual exposure pathways to the total dose over the full simulation horizon are illustrated in Figure 3, which shows that external gamma, plant ingestion, and radon dominate throughout.

Table 5: Total Dose Contributions TDOSE(i,p,t) for Individual Radionuclides and Pathways at t-max-D = 37.65 Years (mSv yr^{-1})

Nuclide	Ground	Inhalation	Radon	Plant	Meat	Milk	Soil	All Pathways
^{40}K	1.432E-01	3.660E-06	0.000E+00	1.398E-01	1.411E-01	5.866E-02	1.586E-04	4.830E-01
^{226}Ra	4.292E-02	2.036E-05	1.783E-01	5.301E-02	3.400E-03	2.696E-03	1.178E-03	2.815E-01
^{232}Th	1.733E-01	6.350E-04	8.629E-03	1.830E-01	1.050E-02	1.277E-02	2.374E-03	3.913E-01
Total	3.595E-01	6.590E-04	1.870E-01	3.759E-01	1.550E-01	7.413E-02	3.711E-03	1.156E+00

Note: Water-Dependent Pathway Contributions were Zero for All Nuclides. All Values in mSv yr^{-1}. From RESRAD-Onsite 7.2 Output File SITE4.RAD

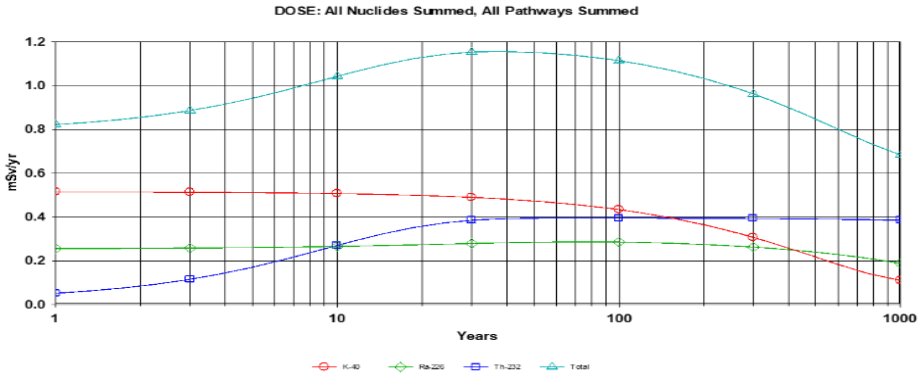

Figure 2: Dose- All Nuclides Summed, All Pathways Summed — Total Radiological Dose (mSv/yr) over 1000 Years at Hongyum Quarry, Mpape (cover depth = 0.00 m). Maximum Dose = 1.156E+00 mSv/yr at t = 37.65 ± 0.08 Years, Exceeding the BRDL of 1.000E+00 mSv/yr

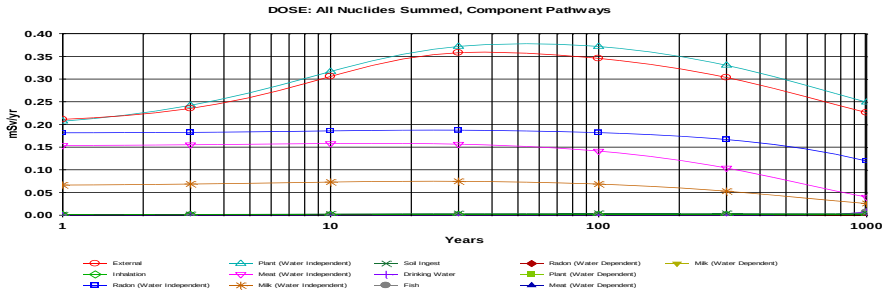

Figure 3: Dose- All Nuclides Summed, Component Pathways — Individual Exposure Pathway Contributions to Total Dose (mSv/yr) Over 1000 Years. External Gamma, Plant Ingestion, and Radon are the Dominant Pathways

Excess Cancer Risk Assessment

The excess cancer risks attributable to each radionuclide and pathway at t = 0 years are presented in Table 6 and illustrated in Figure 4. The total excess cancer risk across all pathways and nuclides was 3.306E-03, which is 11.02 times higher than the WHO- and ICRP-recommended upper limit of 3.00×10^{-4} for members of the public (WHO, 2000; ICRP, 1990). This level of cancer risk is consistent with findings from RESRAD-based assessments at other Nigerian mining and quarry sites (Abdu et al., 2024; Bello et al., 2022; Muhammad et al., 2024). Among the principal radionuclides, ^{40}K was the dominant contributor to total excess cancer risk at 1.952E-03 (59.04% of total), driven primarily by its high activity concentration and its plant ingestion (6.566E-04) and meat ingestion (6.620E-04) pathway risks. ^{226}Ra contributed 7.983E-04 (24.14%), with its radon pathway (6.279E-04) constituting the most significant ^{226}Ra risk route. ^{232}Th contributed 5.560E-04 (16.82%) at t = 0. Within this total, the radon pathway alone — summing ^{222}Rn ($\lambda = 6.519 \times 10^{-5}$ s^{-1}), ^{218}Po ($\lambda = 1.262 \times 10^{-4}$ s^{-1}), ^{214}Pb ($\lambda = 1.596 \times 10^{-4}$ s^{-1}), and ^{214}Bi ($\lambda = 3.122 \times 10^{-4}$ s^{-1}) decay-product inhalation — accounts for 6.411E-04, or 19.4% of the total excess cancer risk, underscoring the importance of including radon decay-product inhalation explicitly in the risk assessment.

Table 6: Excess Cancer Risks CNRS(i,p,t) for Individual Radionuclides and Pathways at t = 0 Years

Nuclide	Ground	Inhalation	Radon	Plant	Meat	Milk	Soil	All Pathways
^{40}K	3.583E-04	8.101E-09	0.000E+00	6.566E-04	6.620E-04	2.752E-04	7.439E-07	1.952E-03
^{226}Ra	1.042E-04	3.948E-08	6.279E-04	5.809E-05	3.633E-06	3.334E-06	1.036E-06	7.983E-04
^{232}Th	2.866E-04	5.132E-07	1.329E-05	2.245E-04	1.284E-05	1.566E-09	2.632E-06	5.560E-04
Total	7.491E-04	5.608E-07	6.411E-04	9.385E-04	6.785E-04	2.942E-04	4.412E-06	3.306E-03

Note: WHO Recommended Limit for Excess Cancer Risk = 3.00 × 10⁻⁴. Total Risk = 3.306E-03 (11.02 × WHO Limit). Radon Pathway Total (6.411E-04) Includes Rn-222, Po-218, Pb-214, Bi-214, and Rn-220 Chain Contributions

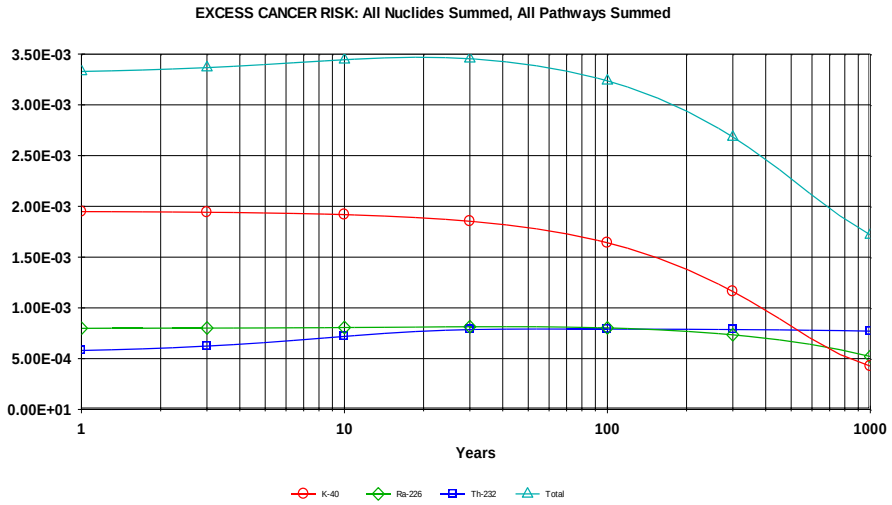

Figure 4: Excess Cancer Risk- All Nuclides Summed, All Pathways Summed — Total Excess Cancer Risk Over 1000 Years at Hongyum Quarry. Peak Risk = 3.306E-03, which is 11.02 Times the WHO-Recommended Limit of 3.00×10^{-4}. K-40 Contributes 59.04% of the Total Risk

Remediation Scenario: 1.25 m Clean Soil Cover

A remediation simulation was performed by introducing a clean soil cover of 1.25 m depth over the contaminated zone (all other parameters unchanged). The results are presented in Table 7 and illustrated in Figure 5. Under the 1.25 m cover scenario, the total dose at t = 0 was reduced from 7.878E-01 mSv/yr (no cover) to 1.367E-01 mSv/yr — a reduction of approximately 82.6%. The dose remained well below the BRDL throughout the simulation: 1.367E-01 mSv/yr at t = 0–1 year, 1.375E-01 mSv/yr at t = 10 years, 1.391E-01 mSv/yr at t = 30 years, 1.448E-01 mSv yr^{-1} at t = 100 years, and 1.544E-01 mSv/yr at t = 300 years.

Table 7: Total Dose Contributions TDOSE(i,p,t) for Individual Radionuclides Under the 1.25 m Clean Soil Cover Remediation Scenario (mSv yr^{-1}, all Pathways Summed)

Time (yr)	^{40}K	^{226}Ra	^{232}Th	Total
0	2.114E-07	1.367E-01	7.863E-09	1.367E-01
1	2.133E-07	1.368E-01	4.541E-08	1.368E-01
10	2.172E-07	1.370E-01	1.782E-07	1.370E-01
30	2.314E-07	1.375E-01	6.957E-07	1.375E-01
100	2.772E-07	1.391E-01	1.353E-06	1.391E-01
300	5.219E-07	1.448E-01	2.657E-06	1.448E-01
1000	3.181E-06	1.544E-01	1.653E-05	1.544E-01

Note: Values are TDOSE(i,p,t), all Pathways Summed, from RESRAD-Onsite 7.2 Output (Cover Scenario, Cover Depth = 1.25 m), File SITE1-QUARRY020626.RAD, Pages 9–10. BRDL = 1.000 mSv/yr. Maximum Total Dose = 3.742E-01 mSv/yr at t = 1000 Years, Remaining Below the BRDL Throughout the Simulation

The maximum dose under the cover scenario was 3.742E-01 mSv/yr at t = 1000 years — the end of the simulation horizon. Crucially, even at the peak, the dose remained well below the BRDL of 1.000E+00 mSv/yr. The gradual rise from year 300 onwards reflects slow leaching and migration of ^{232}Th progeny through the cover layer over centuries as radionuclide retardation is eventually overcome by continued transport. Nevertheless, the 1.25 m cover effectively suppresses external gamma radiation and radon emanation during the critical near-term period (0–300 years), when community radiological risk is highest. This finding is consistent with international radiological clean-up practice (EPA, 2014; Walker, 2013) and with analogous studies at South African mine tailings (Njinga & Tshivhase, 2018). The corresponding excess cancer risks under the 1.25 m cover scenario are summarised in Table 8, and the total dose is summarised in Table 7. The total excess cancer risk was reduced from 3.306E-03 (11.02× WHO limit) under the unmitigated condition to 4.795E-04 at t = 0 years under the cover scenario — a reduction of 85.5%. However, a critical finding is that the cancer risk continues to exceed the WHO-recommended upper limit of 3.00×10^{-4} throughout the simulation horizon. At t = 0, the cover risk (4.795E-04) remains 1.60× the WHO limit. This is entirely attributable to ^{226}Ra-driven radon inhalation: unlike external gamma irradiation and ingestion pathways — which are effectively eliminated by the physical soil barrier — radon gas migrates upward through the cover and contributes to inhalation exposure at the surface. This radon breakthrough effect is well documented in the cover-system literature (Njinga & Tshivhase, 2018; Abdu et al., 2024) and explains the persistence of above-limit risk despite the dramatic overall reduction. The risk increases further to 1.028E-03 at t = 1000 years (3.43× WHO limit) as ^{232}Th decay chain progeny and residual ^{226}Ra reach the surface through long-term transport. These findings indicate that while the 1.25 m clean soil cover constitutes a necessary and effective first remediation step — achieving an 85.5% reduction in cancer risk — it is insufficient alone to bring the site within the WHO acceptable cancer risk threshold. Supplementary measures such as a radon-attenuating cover material, increased cover thickness, or sub-cover ventilation barriers warrant further investigation for this site.

Table 8: Total Excess Cancer Risk CNRSI(i, all Pathways, t) for Initially Existent Radionuclides Under the 1.25 m Clean Soil Cover Remediation Scenario

Time (yr)	^{40}K	^{226}Ra	^{232}Th	Total
0	5.809E-10	4.795E-04	1.984E-09	4.795E-04
1	5.862E-10	4.798E-04	2.092E-09	4.798E-04
10	6.358E-10	4.823E-04	2.892E-09	4.823E-04
30	7.618E-10	4.878E-04	3.857E-09	4.878E-04
100	1.434E-09	5.078E-04	7.368E-09	5.078E-04
300	8.741E-09	5.337E-04	4.586E-08	5.338E-04
1000	2.953E-04	4.561E-04	2.770E-04	1.028E-03

Note: Values are CNRSI(i, all Pathways, t) from RESRAD-Onsite 7.2 Output (Cover Scenario, Cover Depth = 1.25 m). ^{232}Th Values Include Contributions from Decay Daughters Ra-228 and Th-228. WHO Recommended Upper Limit for Excess Lifetime Cancer Risk = 3.00×10^{-4}

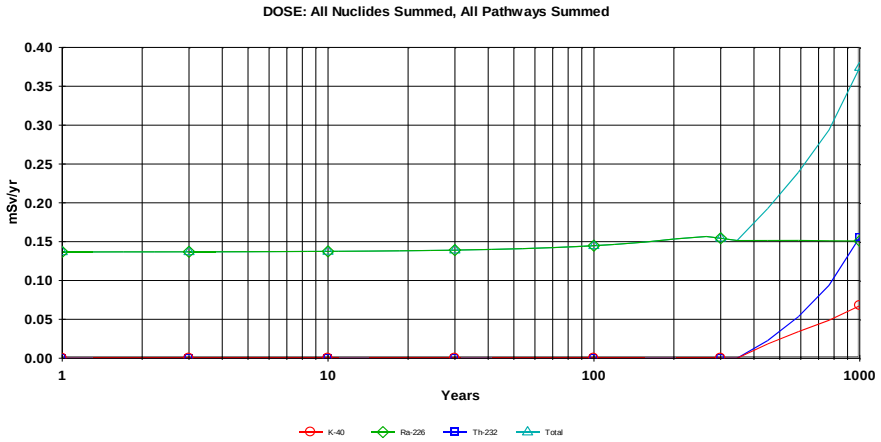

Figure 5: Dose- All Nuclides Summed, All Pathways Summed — 1.25 m Clean Cover Scenario. Total Dose Maintained Well Below BRDL (1.000E+00 mSv yr^{-1}) Throughout the 1000-year Simulation, Peaking at 3.742E-01 mSv yr^{-1} at t = 1000 Years

CONCLUSION

This study applied the RESRAD-Onsite 7.2 code to conduct a long-term radiological dose and cancer risk assessment at Hongyum Quarry, Mpape, FCT Abuja, Nigeria, which is among the first dedicated assessments of this nature for this site. Activity concentrations measured by NaI(Tl) gamma spectrometry yielded mean values of 930.57 ± 61.89 Bq kg^{-1} (^{40}K), 25.34 ± 4.32 Bq kg^{-1} (^{226}Ra), and 76.28 ± 4.81 Bq kg^{-1} (^{232}Th), with ^{40}K and ^{232}Th exceeding UNSCEAR (2000) world average values at all six quarry sampling points.

The maximum total radiological dose of 1.156E+00 mSv yr^{-1} was attained at t = 37.65 ± 0.08 years, exceeding the BRDL of 1.000E+00 mSv yr^{-1}. At t = 0, the total dose was 7.878E-01 mSv yr^{-1}. ^{40}K was the dominant dose contributor at both t = 0 (65.44%) and t-max-D (41.79%), with ^{232}Th's contribution rising substantially over time due to decay chain progeny ingrowth. External gamma, plant ingestion, and radon were the dominant exposure pathways. The total excess cancer risk at t = 0 was 3.306E-03, which is 11.02 times higher than the WHO recommended limit of 3.00×10^{-4}, confirming an unacceptable radiological cancer burden. ^{40}K contributed 59.04% of this risk, primarily through food ingestion pathways.

A 1.25 m clean soil cover reduced the total dose from 7.878E-01 mSv yr^{-1} to 1.367E-01 mSv yr^{-1} at t = 0, with the dose remaining well below the BRDL throughout the 1000-year simulation and peaking at only 3.742E-01 mSv yr^{-1} at t = 1000 years. While this demonstrates that a 1.25 m clean soil cover is an effective first remediation step — reducing total dose by 82.6% and total excess cancer risk by 85.5% — the cancer risk remains above the WHO-recommended upper limit of 3.00×10^{-4} throughout the simulation horizon (1.60× limit at t = 0; 3.43× at t = 1000 years), primarily driven by ^{226}Ra-sourced radon breakthrough through the cover. The cover eliminates external gamma and ingestion pathway exposure but cannot suppress radon gas migration. Supplementary radon attenuation measures are therefore recommended alongside the soil cover. These findings provide a scientific basis for remediation planning and underscore the need for periodic radiological assessments at quarry and mining sites in Nigeria, in compliance with NNRA (2012) regulations.

ACKNOWLEDGEMENT

The authors are grateful to Prof. D. J. Adeyemo for reviewing and approving the laboratory procedures and results carried out at the Centre for Energy Research and Training (CERT), Ahmadu Bello University, Zaria, Nigeria.

CONFLICT OF INTEREST

No potential conflict of interest relevant to this article was reported.

SOURCES OF FUNDING

The authors declare that no funds, grants, or other support were received during the preparation of this manuscript.

ETHICAL STATEMENT

This article does not contain any studies with human participants or animals performed by any of the authors.

DATA AVAILABILITY

The data that support the findings of this study are available from the corresponding author upon reasonable request.

REFERENCES

Abdu, N. M., Aznan, F. I., & Garba, N. N. (2024). RESRAD-ONSITE simulation to evaluate the effect of contamination thickness in determining the dose and excess lifetime cancer risk due to tin mining activities in Nigeria. Radiation Effects and Defects in Solids. https://doi.org/10.1080/10420150.2024.2305876

Bellamy, M., Finklea, L., Dolislager, F., & Eckerman, K. (2014). Area correction factors for contaminated soil for use in risk and dose assessment models (ORNL/TM-2013/00). Oak Ridge National Laboratory.

Bello, S., Garba, N. N., Muhammad, B. G., & Simon, J. (2022). Application of RESRAD and ERICA tools to estimate dose and cancer risk for artisanal gold mining in Nigeria. Journal of Environmental Radioactivity, 251–252, 106932. https://doi.org/10.1016/j.jenvrad.2022.106932

Clapp, R. B., & Hornberger, G. M. (1978). Empirical equations for some soil hydraulic properties. Water Resources Research, 14(4), 601–604. https://doi.org/10.1029/WR014I004P00601

Daburum, N. H., Mallo, Y. I., & Akila, S. (2023). Assessment of background and soil dumpsites radioactivity in Plateau State, Nigeria. African Journal of Environment and Natural Science Research, 6, 143–157. https://doi.org/10.52589/AJENSR-QQEZNFK7

EPA. (2014). Radiation risk assessment at CERCLA sites (Office of Solid Waste and Emergency Response Memorandum 9285.6-20). U.S. Environmental Protection Agency.

Farai, I. (2007). Activity concentrations of 226Ra, 228Th, and 40K in different food crops from a high background radiation area in Bitsichi, Jos Plateau, Nigeria. Radiation and Environmental Biophysics. https://doi.org/10.1007/S00411-006-0085-9

Gil-García, C., Tagami, K., Uchida, S., Rigol, A., & Vidal, M. (2009). New best estimates for radionuclide solid-liquid distribution coefficients in soils. Part 3: Miscellany of radionuclides (Cd, Co, Ni, Zn, I, Se, Sb, Pu, Am, and others). Journal of Environmental Radioactivity, 100(9), 704–715. https://doi.org/10.1016/j.jenvrad.2008.12.001

Girigisu, S., Ibeanu, I. G. E., Adeyemo, D. J., Onoja, R. A., Bappah, I. A., & Okoh, S. (2013). Scholars Research Library Journal Archives of Applied Science Research, 5, 204–210.

IAEA. (1989). Measurement of radionuclides in food and the environment: A guidebook (Technical Reports Series No. 295). International Atomic Energy Agency.

ICRP. (1990). 1990 recommendations of the International Commission on Radiological Protection (ICRP Publication 60). Pergamon Press.

ICRP. (2007). The 2007 recommendations of the International Commission on Radiological Protection (ICRP Publication 103). Annals of the ICRP, 37(2–4), 1–332. https://doi.org/10.1016/j.icrp.2007.10.003

ICRP. (2008). Nuclear decay data for dosimetric calculations (ICRP Publication 107). Annals of the ICRP, 38(3). Elsevier.

Jegede, D. O., Afolabi, T. A., & Agunbiade, F. O. (2025). Spatial distribution and radiological hazards assessment of naturally occurring radionuclide materials in soil from quarry sites in Ogun State, Nigeria. Environmental Monitoring and Assessment, 197, 575. https://doi.org/10.1007/s10661-025-13988-6

Muhammad, A. N., Ismail, A. F., & Garba, N. N. (2024). Natural radioactivity in food crops and soil and estimation of the concomitant dose from tin mining areas in Nigeria. Journal of Taibah University for Science, 19, Article 2366507. https://doi.org/10.1080/16583655.2024.2366507

NAGIS. (2018). Map of Mpape Quarry, Bwari Area Council, FCT Abuja. National Geographic Information System.

Njinga, R. L., & Tshivhase, V. M. (2018). Use of RESRAD-Onsite 7.2 code to assess environmental risk around Tudor Shaft mine tailing sites. Environment and Natural Resources Research, 8(3), 138–147.

NNRA. (2012). Basic ionizing radiation regulations. Nigerian Nuclear Regulatory Authority.

Ofomola, O. M., Ugbede, F. O., & Anomohanran, O. (2023). Environmental risk assessment of background radiation, natural radioactivity and toxic elements in rocks and soils of Nkalagu quarry, Southeastern Nigeria. Journal of Hazardous Materials Advances. https://doi.org/10.1016/j.hazadv.2023.100288

Ojo, E. O., Abdulahi, H. A., Adelowo, A. A., Tine, A. A., Dauda, A. K., Shittu, H. O., Aliyu, A., & Egga, A. A. (2024). Radiological assessment of background radiation and its associated risk in Junior Secondary School Idu-Koro Abuja, Nigeria. Nigerian Journal of Physics, 33(2), 70–74.

Omeiza, A. E., Danladi, E., & Musa, A. (2022). Assessment of air quality around quarry sites in Mpape, Bwari Area Council, FCT Abuja. International Journal of Scientific and Research Publications, 12(4), 212–219. https://doi.org/10.29322/IJSRP.12.04.2022.p12427

UNSCEAR. (2000). Sources and effects of ionizing radiation: 2000 report to the General Assembly. United Nations.

Walker, S. A. (2013). Revisions to US EPA Superfund risk and dose assessment models and guidance. WM Symposia, Tempe, AZ.

WHO. (2000). Guidelines for drinking-water quality (2nd ed., Vol. 2: Health criteria and other supporting information). World Health Organization.

Yu, C. (1987). Modelling of low-level-waste disposal for environmental impact analysis (CONF-870306—70). Argonne National Laboratory.

Yu, C. (1999). RESRAD family of codes and comparison with other codes for decontamination and restoration of nuclear facilities (Chapter 11, pp. 207–231).

Yu, C., Orlandini, K. A., Cheng, J. J., & Biwer, B. M. (2001a). Assessing the impact of hazardous constituents on the mobilization, transport, and fate of radionuclides in RCRA waste disposal units (ANL/EAD/TM-93). Argonne National Laboratory.

Yu, C., Zielen, A. J., Cheng, J. J., LePoire, D. J., Gnanapragasam, E., Kamboj, S., Arnish, J., Wallo, A., Williams, W. A., & Peterson, H. (2001b). User's manual for RESRAD version 6 (ANL/EAD-4). Argonne National Laboratory, U.S. Department of Energy.